Advanced Ceramics Progress: Vol. 9, No. 2, (Spring 2023) 45-52

Materials and Energy Research Center
MERC

Contents lists available at ACERP

Advanced Ceramics Progress

Journal Homepage: www.acerp.ir

Original Research Article

Characterization and Magnetic Properties of $CoFe_2O_4$ Nanoparticles Synthesized under Gas Atmosphere: Effect of Ferrofluid Concentration on Hyperthermia Properties

Kamran Heydaryan [a], Mohammad Almasi Kashi [a, b, *]

[a] *PhD, Institute of Nanoscience and Nanotechnology, University of Kashan, Kashan 87317, Iran*
[b] *Professor, Department of Physics, University of Kashan, Kashan 87317, Iran*

* Corresponding Author Email: almac@kashanu.ac.ir (M. Almasi Kashi)

URL: https://www.acerp.ir/article_176464.html

ARTICLE INFO

Article History:

Received 16 June 2023
Received in revised form 19 July 2023
Accepted 30 July 2023

Keywords:

Magnetic Nanoparticles
$CoFe_2O_4$
Superparamagnetic
Specific Absorption Rate
Magnetic Hyperthermia
Gas Atmosphere

ABSTRACT

Magnetic hyperthermia (MH) is a promising cancer treatment approach that utilizes magnetic nanoparticles with unique properties such as higher penetration depth and precise thermal control that make them effective for cancer treatment. In addition, the sensitivity of cancer cells to heat and role of magnetic nanoparticles proved to be very effective in combined treatments. Here, $CoFe_2O_4$ nanoparticles are synthesized using a co-precipitation method under gas atmosphere during the synthesis process. The characteristics and properties of the synthesized nanoparticles are investigated using XRD, FESEM, and vibrating sample magnetometer (VSM) analyses. The XRD results confirm the formation of cobalt nanoparticles. The FESEM investigations reveal that nanoparticles have uniform surface morphology and spherical shape. The VSM results show that the $CoFe_2O_4$ nanoparticles possess superparamagnetic properties as confirmed by FORC analysis. Under the gas atmosphere, saturation magnetization (M_s) and coercivity (H_c) of the $CoFe_2O_4$ nanoparticles are obtained as 41.5 emu/g and 34.1 Oe, respectively, while these values in the nanoparticles synthesized without the gas atmosphere are calculated as M_s = 33.8 emu/g and H_c = 42.3 Oe. The MH of the $CoFe_2O_4$ nanoparticles is measured by preparing concentrations of 1, 3, and 5 mg/ml of the nanoparticles under the magnetic field of 400 Oe at the frequency of 400 kHz. The results show that the highest MH is achieved at the concentration of 3 mg/ml, and the specific loss power (SLP) value is measured as 190.3 W/g. Overall, these findings confirm that the co-precipitation method is an effective approach to the synthesis of biocompatible $CoFe_2O_4$ nanoparticles which is in line with the results from MTT analysis, having desirable properties for various applications, especially for MH.

https://doi.org/10.30501/acp.2023.402618.1126

1. INTRODUCTION

Hyperthermia can be classified into several types based on its heat source. Magnetic hyperthermia (MH) is a promising cancer treatment approach that uses magnetic nanoparticles as the sources of heat generation in tumor tissues [1,2]. It offers several advantages over other treatment modalities that are listed in the following: higher penetration depth of alternating magnetic fields than other mechanisms (e.g., light or ultrasound) that allows access to deeper tissues, use of nanoparticles in a wide range of concentrations and their retention in the

Please cite this article as: Heydaryan, K., Almasi Kashi, M., "Characterization and Magnetic Properties of $CoFe_2O_4$ Nanoparticles Synthesized under Gas Atmosphere: Effect of Ferrofluid Concentration on Hyperthermia Properties", ***Advanced Ceramics Progress***, Vol. 9, No. 2, (2023), 45-52. https://doi.org/10.30501/acp.2023.402618.1126

tumor site for repeated treatment sessions, size-dependent magnetic properties that facilitate control and tuning of the heating level, precise control of the nanoparticle size, morphology, and surface modification for different purposes including biocompatibility, ability to provide chemical groups for attaching biological molecules, and minimization of blood protein adsorption. Application of magnetic nanoparticles for hyperthermia cancer therapy is highly promising due to their excellent temperature homogeneity [3-7]. Additionally, they can be simultaneously used in combinatorial therapies. One of these approaches is targeted drug delivery combined with hyperthermia in which the drugs are attached to the surface of nanoparticles as the carriers and delivered to the target tissue [8,9]. A variety of cancer imaging techniques and nano-platforms have been recently used for cancer diagnosis in order to monitor treatment [10,11].

In recent years, different methods have been developed for cancer treatment. These methods are classified into two categories: a) traditional methods such as surgery, chemotherapy, and radiation therapy, and b) advanced methods such as gene therapy, hormone therapy, photodynamic therapy, and hyperthermia therapy (or thermal therapy) [12-14]. In medical science, hyperthermia therapy is referred to as a cancer treatment method in which cancerous tissues are exposed to a temperature increase above the physiological body temperature (37 °C) up to about 6-8 °C. One of the prominent features of the cancer cells, compared to the healthy ones, is their sensitivity and vulnerability to heat, and a temperature increase of more than 6 °C can completely destroy them [15-18]. The sensitivity of the cancer cells to heat results from lack of oxygen caused by poor blood flow in the tumor area. Healthy cells can organize blood flow and dissipate excess heat through the vascular network around them in the convection and diffusion phenomenon while the cancer cells have less ability to expand the vascular network. As a result, blood flow decreases and the tissue becomes overheated (more than 42 °C). In addition, the survival of the tumor cells significantly decreases in the range of 41-47 °C while the healthy cells are hardly affected by this temperature increase [15,16,19].

Due to their small size or high surface area, nanomaterials, especially those with sizes ranging from 1 to 100 nanometers, are characterized by unique optical, electrical, catalytic, thermal, and magnetic properties [20-28]. Magnetic nanoparticles have been used in a wide range of applications because they can be easily separated under an external magnetic field and designed for various purposes such as the advanced material synthesis, magnetic enhancement imaging, and controlled heat imaging [29-31]. Generally, magnetic nanoparticles are composed of magnetic elements such as iron, cobalt, nickel, and their chemical compounds. Among various types of the magnetic nanoparticles, ferrite nanoparticles with superparamagnetic properties have been frequently referred to as the efficient magnetic nanomaterials that are suitable for various applications [6,31-33]. Ferrite nanoparticles have interesting properties such as non-toxicity, biocompatibility, chemical stability, and high magnetic reversibility [34-37]. Cobalt ferrite nanoparticles have a high potential for targeted drug delivery and MRI and for this reason, they have received considerable attention in recent decades. Owing to their attractive magnetic properties, cobalt ferrite nanoparticles have high potential in MH therapy [31,38-40].

Magnetic nanoparticles can be synthesized by physical and chemical methods among which, the co-precipitation method is one of the cost-effective and simple methods. As a disadvantage, some materials in the synthesis through this method do not have uniform quality. One of the ways to control uniformity and proper morphology in the synthesis based on co-precipitation method is to use argon and hydrogen atmosphere that removes excessive oxygen and impurities during the synthesis [41-44]. However, the significant role of the MH properties of cobalt ferrite nanoparticles synthesized by a co-precipitation method under the gas atmosphere has been still neglected.

In this study, the prepared sample was first converted into a stable nanoparticle suspension with a specific concentration. Then, the sample was placed in a MH measurement device where an alternating magnetic field with a specific intensity and frequency was applied, and the temperature increase of the nanoparticle suspension was measured and recorded for one minute. The value of specific loss power (SLP), which indicates the amount of the MH of the nanoparticles in the presence of the magnetic field, was calculated using Equation (1) In this equation, c represents the specific heat capacity of the solvent, m_{MNPs} the mass of the magnetic nanoparticles, m_f the mass of the fluid, and $\Delta T/\Delta t$ the initial slope of the temperature-time curve [45].

$$SLP = c\frac{m_f}{m_{MNPs}}\frac{\Delta T}{\Delta t} \quad (1)$$

2. MATERIALS AND METHODS

2.1. Synthesis of $CoFe_2O_4$ Nanoparticles

For the synthesis of $CoFe_2O_4$, 10 ml of 0.5 M $FeCl_3.6H_2O$ and 6 ml of 0.4 M $CoCl_2.6H_2O$ were mixed in a three-necked flask and placed on a temperature-controlled heater mantel. The mixture was then heated to 85 °C under the gas atmosphere (85 % argon + 15 % hydrogen) [46,47]. During the heating process, the pH of the medium reached about 12 by adding NaOH solution drop by drop. The solution was stirred for 60 min at 85 °C and then, the obtained precipitate was cooled down to room

temperature. Finally, the precipitate was washed five times with ethanol and deionized water using a centrifuge. The schematic of the synthesis steps is shown in Figure 1.

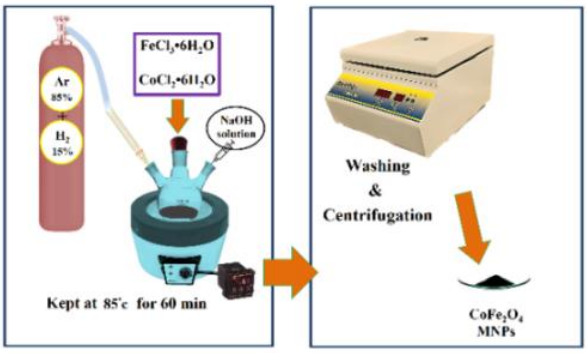

Figure 1. Schematic representation of the preparation process of $CoFe_2O_4$ nanoparticles using a co-precipitation method under gas atmosphere

2.2. Characterizations

A Field-Emission Scanning Electron Microscope (FESEM, TESCAN, Czech) was used to investigate the morphology of $CoFe_2O_4$ synthesized with different surfactants. Then, X-Ray Diffraction (XRD; Philips, X'Pert Pro, λ = 0.154 nm) analysis was done to study the crystal structure of the $CoFe_2O_4$. The magnetic properties were then investigated at room temperature by measuring the hysteresis curves (applied magnetic field: ±10000 Oe) and doing FORC analysis using a vibrating sample magnetometer (VSM, MDK Co.) equipped with FORC software.

MH value of the $CoFe_2O_4$ was evaluated by measuring their heating efficiency using an alternating magnetic field with the intensity of 400 Oe at the frequency of 400 kHz. For this purpose, a hyperthermia device (Magnetic DaneshPajoh Kashan Co.) was used. The SLP value of the prepared ferrofluids (containing $CoFe_2O_4$ nanoparticles with concentrations of 1, 3, and 5 mg/ml in deionized water) was calculated through Equation (1).

3. RESULTS AND DISCUSSION

3.1. XRD Results

The XRD pattern of the synthesized $CoFe_2O_4$ is shown in Figure 2. In general, the XRD peaks at 2θ = 18.2°, 29.9°, 35.4°, 36.8°, 42.9°, 53.2°, 56.6°, 62.4°, and 73.6°, respectively, can be indexed to (111), (220), (311), (222), (400), (442), (511), (440), and (533) reflections of face-centered cubic $CoFe_2O_4$ crystal structure (JCPDS card no. 00-002-1045). The absence of other peaks is indicative of the high purity of the synthesized sample. The average crystallite size (d_{cs}) was estimated along the preferential orientation using Scherrer equation [48]:

$$d_{CS} = \frac{K\lambda}{\beta\cos\theta} \quad (2)$$

where K is the shape factor (K = 0.9), λ the X-ray wavelength, β (in terms of radian) the full width at half maximum, and θ the diffraction angle. Accordingly, the value of d_{cs} of $CoFe_2O_4$ was obtained as d 21.6 nm [49-54].

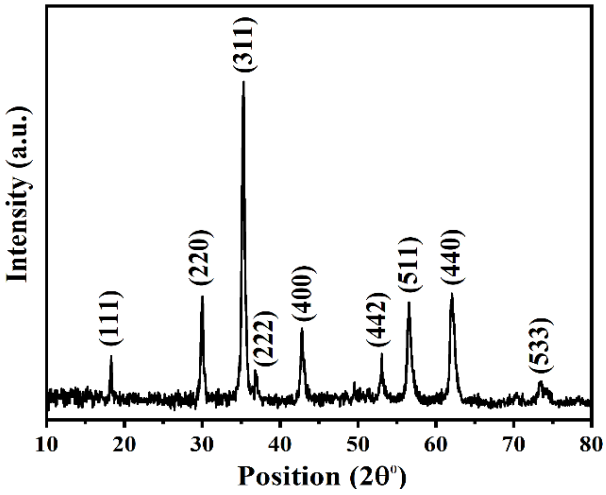

Figure 2. XRD pattern of $CoFe_2O_4$

3.2. FESEM Results

Figure 3 demonstrates the FESEM image of the $CoFe_2O_4$ nanoparticles. The synthesized cobalt ferrite nanoparticles have spherical morphology and suitable uniformity, one of the effective factors on the magnetic heat enhancement of magnetic nanoparticles. As observed in the inset of Figure 3, the size distribution of the $CoFe_2O_4$ nanoparticles was obtained using FESEM images and Digimizer software. The size of the $CoFe_2O_4$ nanoparticles is in the range of 10 to 38 nm with the average size of 24 nm, indicating the formation of superparamagnetic nanoparticles.

3.3. Hysteresis Curve and FORC Results

The room temperature hysteresis curve of the synthesized $CoFe_2O_4$ nanoparticles is illustrated in Figure 4. To study the magnetic properties of cobalt ferrite nanoparticles synthesized under gas atmosphere (S1) and without gas atmosphere (S2), a magnetic field in the range of -10 kOe to +10 kOe was applied to the samples in order to obtain the magnetic parameters. The saturation magnetization (M_S) and coercivity (H_C) values of the samples S1 and S2 are found to be 41.5 emu/g and 34.1 Oe and 33.8 emu/g and 42.3 Oe, respectively. It is inferred that the gas atmosphere probably prevents the formation of oxide impurities in the cobalt ferrite nanoparticles, thus enhancing M_S value up to about 22 % (from 33.8 to 41.5 emu/g). These nanoparticles are considered as superparamagnetic materials due to their

low coercivity. In addition to generating magnetic heat, this property of nanoparticles can also be used to increase the image contrast in the MRI since these nanoparticles do not have any harmful effects on the human body. Figure 4 shows the hysteresis curve of $CoFe_2O_4$ nanoparticles, which shows the superparamagnetic nature of cobalt ferrite nanoparticles due to its very narrow width (close to zero).

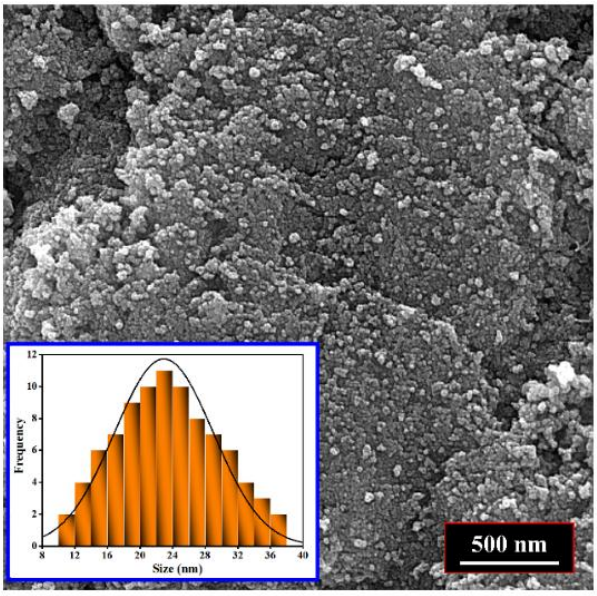

Figure 3. FESEM image of $CoFe_2O_4$. The inset represents the corresponding size distribution

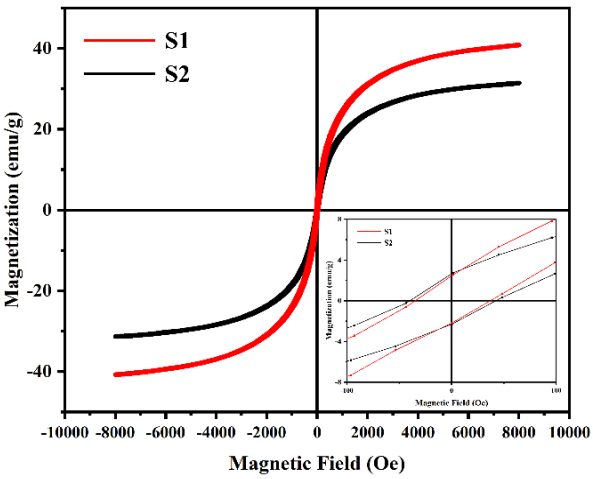

Figure 4. Hysteresis curves of the $CoFe_2O_4$ nanoparticles synthesized under gas atmosphere (S1) and without gas atmosphere (S2). The inset shows the details of the curves.

The FORC analysis was carried out by initially intensifying the magnetic field (H) applied to the sample up to its saturation field, followed by decreasing it by a reverse field (H_r). During this process, magnetization M (H, H_r) was measured. Accordingly, sets of FORCs were plotted. The magnetic field ranged from –750 to +750 Oe, having a reversal step of 30 Oe. The FORC diagram depicted in Figure 5 shows a coercive field distribution ranging between 0 and 110 Oe. This may also indicate the relatively high contribution of the superparamagnetic $CoFe_2O_4$ nanoparticles due to their small average diameter. In the FORC diagram, the extent of the coercive field and magnetostatic interactions can be extracted, showing the uniformity and distribution of the nanoparticle size. The mild coercive field distribution around the origin of the graph (H_c^{FORC} < 110 Oe) is attributed to the quasi-superparamagnetic behavior of the nanoparticles [55].

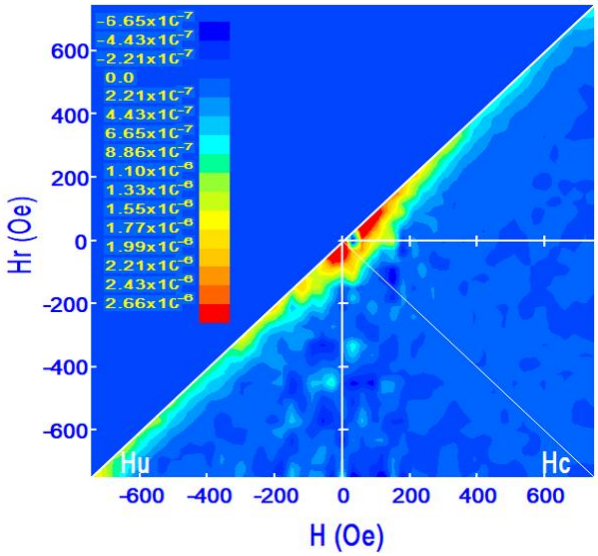

Figure 5. FORC diagram of $CoFe_2O_4$ nanoparticles

3.4. MH Measurements and MTT Results

In the measurements of the MH which ultimately leads to the calculation of SLP, ferrofluids containing cobalt ferrite nanoparticles with the concentrations of 1, 3, and 5 mg/ml were prepared in aqueous medium. An ultrasonic bath was then used to disperse nanoparticles in water, and the solutions were placed in the bath for 30 min. The hyperthermia properties of the nanoparticles were measured using a MH machine (MDK, Iran). The ferrofluids of the samples were subjected to an alternating magnetic field with the frequency of 400 kHz and field intensity of 400 Oe in the device. Figure 6a shows the ΔT with respect to the time of nanoparticles in a period of 5 min. The SLP values were calculated using Equation 1 by considering the temperature increase value measured in a one-minute period.

Figure 6b shows the amounts of the SLP of the $CoFe_2O_4$ nanoparticles with the concentrations of 1, 3, and 5 mg/ml, and the highest amount equals 190.3 W/g at the concentration of 3 mg/ml. A comparison of the heat

dissipation power of the samples with different concentrations shows that the decrease in concentration (from 5 to 3 mg/ml) causes an increase in the heat produced by the ferrofluid.

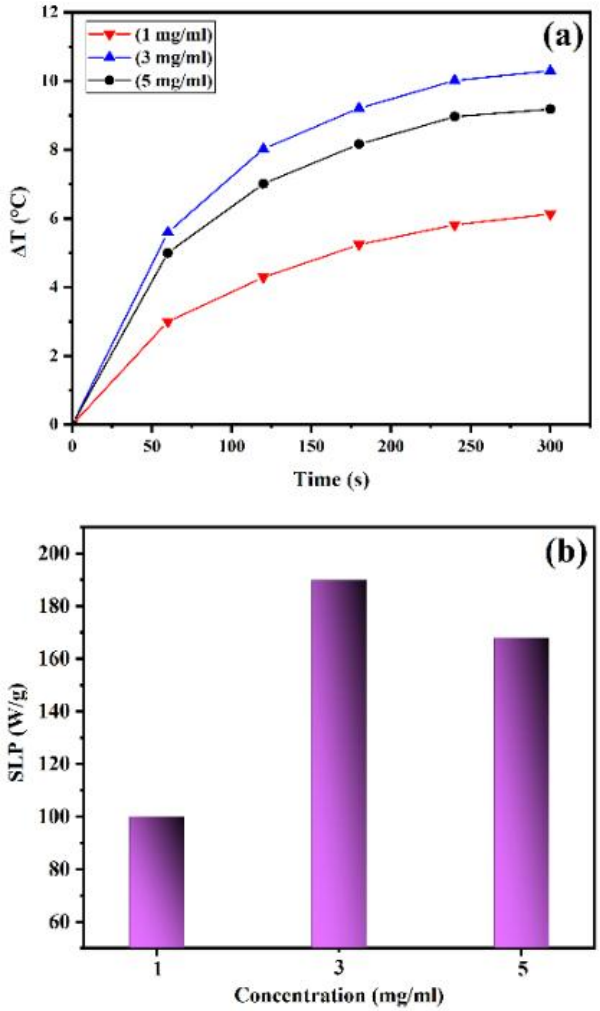

Figure 6. (a) Variation of ΔT with respect to time for ferrofluids of $CoFe_2O_4$ nanoparticles and (b) different concentrations of ferrofluids (1, 3, and 5 mg/ml)

As the concentration decreases, the amount of nanoparticles dissolved in the solution decreases. Meanwhile, the solution becomes less viscous, and the distance between the nanoparticles increases. This, in turn, lessens the interaction between the nanoparticles, thus making them have less obstacles against their physical rotation in the fluid. As a result, they can convert more amount of the absorbed electromagnetic energy into heat due to their higher and faster rotation movements that eventually increases the SLP. It should be noted that changing the concentration can affect the Brownian relaxation mechanism, which is related to the rotation of nanoparticles. In fact, the Néel mechanism is related to the rotation of the moments inside the nanoparticles, hence independent of the surrounding environment of the nanoparticles. Finally, at the concentration of 3 mg/ml, the effect of Néel and Brownian mechanisms reaches its optimal state, and the effect of these two mechanisms leads to the highest SLP at this concentration. Other effective factors that determine the SLP value are the characteristics of the measuring device such as the frequency and intensity of the field [56,57].

Figure 7 illustrates the MTT assay results obtained from the $CoFe_2O_4$ nanoparticles after 24, 48, and 72 h. According to findings, the cell viability of the L929 cells remains high (> 85 %) in the presence of these nanoparticles. Overall, it can be concluded that $CoFe_2O_4$ nanoparticles with high SLPs do not have a significant cytotoxic effect on the L929 cells, hence suitable for MH therapy.

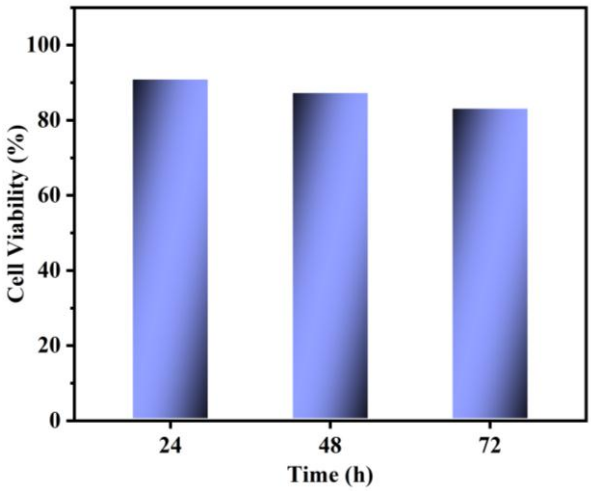

Figure 7. MTT assay results of $CoFe_2O_4$ nanoparticles for different times

4. CONCLUSION

In conclusion, $CoFe_2O_4$ nanoparticles were synthesized in this study based on a co-precipitation method under gas atmosphere (85 % argon + 15 % hydrogen). The formation of cobalt nanoparticles was confirmed based on the XRD results. The FESEM investigations showed that the surface morphology of the $CoFe_2O_4$ nanoparticles was uniform. In addition, according to the FESEM images, the nanoparticles under study had spherical morphology. The results of the hysteresis curve showed that $CoFe_2O_4$ nanoparticles were superparamagnetic in nature. The gas atmosphere played a constructive role in enhancing the magnetic properties by increasing the M_s value up to about 22 %. Further, the FORC analysis confirmed the superparamagnetic contribution of the nanoparticles. Investigations of the

magnetic heat enhancement at the concentrations of 1, 3, and 5 mg/ml in aqueous medium confirmed that the suitable concentration for the highest SLP was 3 mg/ml for biocompatible cobalt ferrite nanoparticles. The synthesized nanoparticles have a high potential for drug delivery and MRI in future works.

ACKNOWLEDGEMENT

The authors gratefully acknowledge University of Kashan for providing the financial support of this work by Grant No. 159023/89.

REFERENCES

1. Zhang, J. Z., Tang, H., Chen, X. Z., Su, Q., Xi, W. S., Liu, Y. Y., Liu, Y., Cao, A., Wang, H., "In vivo fate of Ag_2Te quantum dot and comparison with other NIR-II silver chalcogenide quantum dots", ***Journal of Nanoparticle Research***, Vol. 22, No. 9, (2020), 287. https://doi.org/10.1007/s11051-020-04992-7
2. Ferreira, I. N., Isikawa, M. M., Nunes, L. H. S., Micheletto, M. C., Guidelli, E. J., "Magnetic nanoparticles covered with polycyclic aromatic hydrocarbons as singlet oxygen carriers for combining photodynamic therapy and magnetic hyperthermia", ***Journal of Photochemistry and Photobiology A: Chemistry***, Vol. 444, (2023), 114902. https://doi.org/10.1016/j.jphotochem.2023.114902
3. Myrovali, E., Papadopoulos, K., Charalampous, G., Kesapidou, P., Vourlias, G., Kehagias, T., Angelakeris, M., Wiedwald, U., "Toward the Separation of Different Heating Mechanisms in Magnetic Particle Hyperthermia", ***ACS Omega***, Vol. 8, No. 14, (2023), 12955-12967. https://doi.org/10.1021/acsomega.2c05962
4. Rossi, L. M., Quach, A. D., Rosenzweig, Z., "Glucose oxidase–magnetite nanoparticle bioconjugate for glucose sensing", ***Analytical and Bioanalytical Chemistry***, Vol. 380, (2004), 606-613. https://doi.org/10.1007/s00216-004-2770-3
5. Zheng, Y., He, J., Li, B., Wu, T., Dai, W., Li, Y., "Research on DC protection strategy in multi-terminal hybrid HVDC system", ***Engineering***, Vol. 7, No. 8, (2021), 1064-1075. https://doi.org/10.1016/j.eng.2021.05.002
6. Laurent, S., Forge, D., Port, M., Roch, A., Robic, C., Vander Elst, L., Muller, R. N., "Magnetic iron oxide nanoparticles: synthesis, stabilization, vectorization, physicochemical characterizations, and biological applications", ***Chemical Reviews***, Vol. 108, No. 6, (2008), 2064-2110. https://doi.org/10.1021/cr068445e
7. Heydaryan, K., Mohammadalizadeh, M., Montazer, A. H., Kashi, M. A., "Reaction time-induced improvement in hyperthermia properties of cobalt ferrite nanoparticles with different sizes", ***Materials Chemistry and Physics***, Vol. 303, (2023), 127773. https://doi.org/10.1016/j.matchemphys.2023.127773
8. Esmaeili, A., Hemami, R., Ghaffari, Y., Abdollahi, S., "A review on evaluation of natural polymers with the approach of drug delivery system using herbal plant microcapsules", ***Journal of Simulation and Analysis of Novel Technologies in Mechanical Engineering***, Vol. 14, No. 2, (2022), 65-77. https://journals.iau.ir/article_693977_aed449699e5f9b7545209fa6f0af9527.pdf
9. Dobson, J., "Magnetic nanoparticles for drug delivery", ***Drug Development Research***, Vol. 67, No. 1, (2006), 55-60. https://doi.org/10.1002/ddr.20067
10. Thorat, N. D., ***Advances in Image-Guided Cancer Nanomedicine***, IOP Publishing Ltd, Bristol, UK, (2022). https://doi.org/10.1088/978-0-7503-3675-8
11. Jadhav, S. A., Somvanshi, S. B., Gawali, S. S., Zakade, K., Jadhav, K. M., "Rare earth-doped mixed Ni–Cu–Zn ferrites as an effective photocatalytic agent for active degradation of Rhodamine B dye", ***Journal of Rare Earths***, (2023). https://doi.org/10.1016/j.jre.2023.03.004
12. Ullah, A., Ullah, N., Nawaz, T., Aziz, T., "Molecular mechanisms of Sanguinarine in cancer prevention and treatment", ***Anti-Cancer Agents in Medicinal Chemistry (Formerly Current Medicinal Chemistry-Anti-Cancer Agents)***, Vol. 23, No. 7, (2023), 765-778. https://doi.org/10.2174/1871520622666220831124321
13. Zhang, J., Wang, S., Zhou, Z., Lei, C., Yu, H., Zeng, C., Xia, X., Qiao, G., Shi, Q., "Unpleasant symptoms of immunotherapy for people with lung cancer: A mixed-method study", ***International Journal of Nursing Studies***, Vol. 139, (2023), 104430. https://doi.org/10.1016/j.ijnurstu.2022.104430
14. Naik, M. M., Vinuth, M., Kumar, V. U., Hemakumar, K. H., Preethi, G., Kumar, M. P., Nagaraju, G., "A facile green synthesis of nickel ferrite nanoparticles using Tamarindus Indica seeds for magnetic and photocatalytic studies", ***Nanotechnology for Environmental Engineering***, Vol. 8, No. 1, (2023), 143-151. https://doi.org/10.1007/s41204-022-00257-x
15. Hishiki, A., Sato, M., Hashimoto, H., "Structure of HIRAN domain of human HLTF bound to duplex DNA provides structural basis for DNA unwinding to initiate replication fork regression", ***The journal of biochemistry***, Vol. 167, No. 6, (2020), 597-602. https://doi.org/10.1093/jb/mvaa008
16. Ahmed, K., Tabuchi, Y., Kondo, T., "Hyperthermia: an effective strategy to induce apoptosis in cancer cells", ***Apoptosis***, Vol. 20, (2015), 1411-1419. https://doi.org/10.1007/s10495-015-1168-3
17. Putri, C. D., Hadi, A. F., Anggraeni, D., Riski, A., "Projection pursuit regression and principal component regression on statistical downscaling using artificial neural network for rainfall prediction in Jember", In ***Journal of Physics: Conference Series***, May 2021, IOP Publishing, Vol. 1872, No. 1, (2021), 012023. https://doi.org/10.1088/1742-6596/1872/1/012023
18. Koroulakis, A., Rice, S. R., DeCesaris, C., Knight, N., Nichols, E. M., "Perceptions and patterns in academic publishing: a survey of United States residents in radiation oncology", ***Advances in Radiation Oncology***, Vol. 5, No. 2, (2020), 146-151. https://doi.org/10.1016/j.adro.2019.09.001
19. Dunne, M., Dou, Y. N., Drake, D. M., Spence, T., Gontijo, S. M., Wells, P. G., Allen, C., "Hyperthermia-mediated drug delivery induces biological effects at the tumor and molecular levels that improve cisplatin efficacy in triple negative breast cancer", ***Journal of Controlled Release***, Vol. 282, (2018), 35-45. https://doi.org/10.1016/j.jconrel.2018.04.029
20. Giannone, G., Santi, M., Ermini, M. L., Cassano, D., Voliani, V., "A cost-effective approach for non-persistent gold nano-architectures production", ***Nanomaterials***, Vol. 10, No. 8, (2020), 1600. https://doi.org/10.3390/nano10081600
21. Kaur, P., Thakur, M., Tondan, D., Bamrah, G. K., Misra, S., Kumar, P., Pandohee, J., Kulshrestha, S., "Nanomaterial conjugated lignocellulosic waste: cost-effective production of sustainable bioenergy using enzymes", ***3 Biotech***, Vol. 11, No. 11, (2021), 480. https://doi.org/10.1007/s13205-021-03002-4
22. Tulinski, M., Jurczyk, M., "Nanomaterials synthesis methods", ***Metrology and Standardization of Nanotechnology, Protocols and Industrial Innovations***, (2017), 75-98. https://doi.org/10.1002/9783527800308.ch4
23. Manivasagan, P., Ashokkumar, S., Manohar, A., Joe, A., Han, H. W., Seo, S. H., Thambi, T., Duong, H. S., Kaushik, N. K., Kim, K. H., Choi, E. H., Jang, E. S., "Biocompatible Calcium Ion-Doped Magnesium Ferrite Nanoparticles as a New Family of Photothermal Therapeutic Materials for Cancer Treatment", ***Pharmaceutics***, Vol. 15, No. 5, (2023), 1555. https://doi.org/10.3390/pharmaceutics15051555
24. Manohar, A., Vijayakanth, V., Vattikuti, S. P., Kim, K. H.,

"Structural, BET and EPR properties of mixed zinc-manganese spinel ferrites nanoparticles for energy storage applications", ***Ceramics International***, Vol. 49, No. 12, (2023), 19717-19727. https://doi.org/10.1016/j.ceramint.2023.03.089

25. Manohar, A., Krishnamoorthi, C. J. M. C., "Low Curie-transition temperature and superparamagnetic nature of Fe_3O_4 nanoparticles prepared by colloidal nanocrystal synthesis", ***Materials Chemistry and Physics***, Vol. 192, (2017), 235-243. https://doi.org/10.1016/j.matchemphys.2017.01.039
26. Manohar, A., Krishnamoorthi, C., "Structural, optical, dielectric and magnetic properties of $CaFe_2O_4$ nanocrystals prepared by solvothermal reflux method", ***Journal of Alloys and Compounds***, Vol. 722, (2017), 818-827. https://doi.org/10.1016/j.jallcom.2017.06.145
27. Manohar, A., Vijayakanth, V., Vattikuti, S. P., Kim, K. H., "A mini-review on AFe_2O_4 (A= Zn, Mg, Mn, Co, Cu, and Ni) nanoparticles: Photocatalytic, magnetic hyperthermia and cytotoxicity study", ***Materials Chemistry and Physics***, Vol. 286, (2022), 126117. https://doi.org/10.1016/j.matchemphys.2022.126117
28. Manohar, A., Vijayakanth, V., Manivasagan, P., Jang, E. S., Hari, B., Gu, M., Kim, K. H., "Investigation on the physico-chemical properties, hyperthermia and cytotoxicity study of magnesium doped manganese ferrite nanoparticles", ***Materials Chemistry and Physics***, Vol. 287, (2022), 126295. https://doi.org/10.1016/j.matchemphys.2022.126295
29. Sperling, R. A., Parak, W. J., "Surface modification, functionalization and bioconjugation of colloidal inorganic nanoparticles", ***Philosophical Transactions of the Royal Society A: Mathematical, Physical and Engineering Sciences***, Vol. 368, No. 1915, (2010), 1333-1383. https://doi.org/10.1098/rsta.2009.0273
30. Derakhti, S., Safiabadi-Tali, S. H., Amoabediny, G., Sheikhpour, M., "Attachment and detachment strategies in microcarrier-based cell culture technology: A comprehensive review", ***Materials Science and Engineering: C***, Vol. 103, (2019), 109782. https://doi.org/10.1016/j.msec.2019.109782
31. Chikawa, J. I., Bandou, M., Tabuchi, K., Tani, K., Saji, H., Takasaki, Y., "Hair growth at a solid-liquid interface as a protein crystal without cell division", ***Progress in Crystal Growth and Characterization of Materials***, Vol. 65, No. 3, (2019), 100452. https://doi.org/10.1016/j.pcrysgrow.2019.04.002
32. Reeves, S. M., Lawal, A., "Characterization and surface impact of paracetamol granules formed by binder dropping", ***Journal of Drug Delivery Science and Technology***, Vol. 61, (2021), 102153. https://doi.org/10.1016/j.jddst.2020.102153
33. Faraji, M., Yamini, Y., Rezaee, M., "Magnetic nanoparticles: synthesis, stabilization, functionalization, characterization, and applications", ***Journal of the Iranian Chemical Society***, Vol. 7, (2010), 1-37. https://doi.org/10.1007/BF03245856
34. Akhtar, S., Slimani, Y., Almessiere, M. A., Baykal, A., Polat, E. G., Caliskan, S., "Influence of Tm and Tb co-substitution on structural and magnetic features of $CoFe_2O_4$ nanospinel ferrites", ***Nano-Structures & Nano-Objects***, Vol. 33, (2023), 100944. https://doi.org/10.1016/j.nanoso.2023.100944
35. Liandi, A. R., Cahyana, A. H., Kusumah, A. J. F., Lupitasari, A., Alfariza, D. N., Nuraini, R., Sari, R. W., Kusumasari, F. C., "Recent trends of spinel ferrites (MFe_2O_4: Mn, Co, Ni, Cu, Zn) applications as an environmentally friendly catalyst in multicomponent reactions: A review", ***Case Studies in Chemical and Environmental Engineering***, (2023), 100303. https://doi.org/10.1016/j.cscee.2023.100303
36. Du, W., Zheng, Y., Liu, X., Cheng, J., Reddy, R. C. K., Zeb, A., Lin, X., Luo, Y., "Oxygen-enriched vacancy spinel MFe_2O_4/carbon (M= Ni, Mn, Co) derived from metal-organic frameworks toward boosting lithium storage", ***Chemical Engineering Journal***, Vol. 451, (2023), 138626. https://doi.org/10.1016/j.cej.2022.138626
37. Salokhe, A., Koli, A., Jadhav, V., Mane-Gavade, S., Supale, A., Dhabbe, R., Yu, X.-Y., Sabale, S., "Magneto-structural and induction heating properties of MFe_2O_4 (M= Co, Mn, Zn) MNPs for magnetic particle hyperthermia application", ***SN Applied Sciences***, Vol. 2, No. 12, (2020), 2017. https://doi.org/10.1007/s42452-020-03865-x
38. Manthiram, A., Fu, Y., Chung, S. H., Zu, C., Su, Y. S., "Rechargeable lithium–sulfur batteries", ***Chemical Reviews***, Vol. 114, No. 23, (2014), 11751-11787. https://doi.org/10.1021/cr500062v
39. Manohar, A., Vijayakanth, V., Vattikuti, S. P., Kim, K. H., "Electrochemical investigation on nickel-doped spinel magnesium ferrite nanoparticles for supercapacitor applications", ***Materials Chemistry and Physics***, Vol. 301, (2023), 127601. https://doi.org/10.1016/j.matchemphys.2023.127601
40. Manohar, A., Vijayakanth, V., Vattikuti, S. P., Kim, K. H., "Electrochemical energy storage and photoelectrochemical performance of $Ni_{1-X}Zn_XFe_2O_4$ nanoparticles", ***Materials Science in Semiconductor Processing***, Vol. 157, (2023), 107338. https://doi.org/10.1016/j.mssp.2023.107338
41. Sartori, K., Cotin, G., Bouillet, C., Halté, V., Bégin-Colin, S., Choueikani, F., Pichon, B. P., "Strong interfacial coupling through exchange interactions in soft/hard core–shell nanoparticles as a function of cationic distribution", ***Nanoscale***, Vol. 11, No. 27, (2019), 12946-12958. https://doi.org/10.1039/C9NR02323B
42. Wang, C., Peng, S., Lacroix, L. M., Sun, S., "Synthesis of high magnetic moment CoFe nanoparticles via interfacial diffusion in core/shell structured Co/Fe nanoparticles", ***Nano Research***, Vol. 2, (2009), 380-385. https://doi.org/10.1007/s12274-009-9037-4
43. Lee, K., Lee, S., Ahn, B., "Understanding high anisotropic magnetism by ultrathin shell layer formation for magnetically hard–soft core–shell nanostructures", ***Chemistry of Materials***, Vol. 31, No. 3, (2019), 728-736. https://doi.org/10.1021/acs.chemmater.8b03591
44. Smith, M., McKeague, M., DeRosa, M. C., "Synthesis, transfer, and characterization of core-shell gold-coated magnetic nanoparticles", ***MethodsX***, Vol. 6, (2019), 333-354. https://doi.org/10.1016/j.mex.2019.02.006
45. Tatarchuk, T., Shyichuk, A., Sojka, Z., Gryboś, J., Naushad, M., Kotsyubynsky, V., Kowalska, M., Kwiatkowska-Marks, S., Danyliuk, N., "Green synthesis, structure, cations distribution and bonding characteristics of superparamagnetic cobalt-zinc ferrites nanoparticles for Pb (II) adsorption and magnetic hyperthermia applications", ***Journal of Molecular Liquids***, Vol. 328, (2021), 115375. https://doi.org/10.1016/j.molliq.2021.115375
46. Ferjaoui, Z., Jamal Al Dine, E., Kulmukhamedova, A., Bezdetnaya, L., Soon Chang, C., Schneider, R., Mutelet, F., Mertz, D., Begin-Colin, S., Quilès, F., "Doxorubicin-loaded thermoresponsive superparamagnetic nanocarriers for controlled drug delivery and magnetic hyperthermia applications", ***ACS Applied Materials & Interfaces***, Vol. 11, No. 34, (2019), 30610-30620. https://doi.org/10.1021/acsami.9b10444
47. Hufschmid, R., Arami, H., Ferguson, R. M., Gonzales, M., Teeman, E., Brush, L. N., Browning, N. D., Krishnan, K. M., "Synthesis of phase-pure and monodisperse iron oxide nanoparticles by thermal decomposition", ***Nanoscale***, Vol. 7, No. 25, (2015), 11142-11154. https://doi.org/10.1039/C5NR01651G
48. Phadatare, M. R., Meshram, J. V., Gurav, K. V., Kim, J. H., Pawar, S. H., "Enhancement of specific absorption rate by exchange coupling of the core–shell structure of magnetic nanoparticles for magnetic hyperthermia", ***Journal of Physics D: Applied Physics***, Vol. 49, No. 9, (2016), 095004. https://doi.org/10.1088/0022-3727/49/9/095004
49. Permien, S., Indris, S., Schürmann, U., Kienle, L., Zander, S., Doyle, S., Bensch, W., "What happens structurally and electronically during the li conversion reaction of $CoFe_2O_4$ nanoparticles: an operando XAS and XRD investigation",

Chemistry of Materials, Vol. 28, No. 2, (2016), 434-444. https://doi.org/10.1021/acs.chemmater.5b01754

50. Bhosale, A. B., Somvanshi, S. B., Murumkar, V. D., Jadhav, K. M., "Influential incorporation of RE metal ion (Dy^{3+}) in yttrium iron garnet (YIG) nanoparticles: Magnetic, electrical and dielectric behaviour", ***Ceramics International***, Vol. 46, No. 10, (2020), 15372-15378. https://doi.org/10.1016/j.ceramint.2020.03.081
51. Somvanshi, S. B., Jadhav, S. A., Khedkar, M. V., Kharat, P. B., More, S. D., Jadhav, K. M., "Structural, thermal, spectral, optical and surface analysis of rare earth metal ion (Gd^{3+}) doped mixed Zn–Mg nano-spinel ferrites", ***Ceramics International***, Vol. 46, No. 9, (2020), 13170-13179. https://doi.org/10.1016/j.ceramint.2020.02.091
52. Bharati, V. A., Somvanshi, S. B., Humbe, A. V., Murumkar, V. D., Sondur, V. V., Jadhav, K. M., "Influence of trivalent Al–Cr co-substitution on the structural, morphological and Mössbauer properties of nickel ferrite nanoparticles", ***Journal of Alloys and Compounds***, Vol. 821, (2020), 153501. https://doi.org/10.1016/j.jallcom.2019.153501
53. Manohar, A., Krishnamoorthi, C., "Photocatalytic study and superparamagnetic nature of Zn-doped $MgFe_2O_4$ colloidal size nanocrystals prepared by solvothermal reflux method", ***Journal of Photochemistry and Photobiology B: Biology***, Vol. 173, (2017), 456-465. https://doi.org/10.1016/j.jphotobiol.2017.06.025
54. Manohar, A., Vijayakanth, V., Vattikuti, S. P., Kim, K. H., "Synthesis and characterization of Mg^{2+} substituted $MnFe_2O_4$ nanoparticles for supercapacitor applications", ***Ceramics International***, Vol. 48, No. 20, (2022), 30695-30703. https://doi.org/10.1016/j.ceramint.2022.07.018
55. Salati, A., Ramazani, A., Kashi, M. A., "Tuning hyperthermia properties of FeNiCo ternary alloy nanoparticles by morphological and magnetic characteristics", ***Journal of Magnetism and Magnetic Materials***, Vol. 498, (2020), 166172. https://doi.org/10.1016/j.jmmm.2019.166172
56. Kötitz, R., Weitschies, W., Trahms, L., Semmler, W., "Investigation of Brownian and Néel relaxation in magnetic fluids", ***Journal of Magnetism and Magnetic Materials***, Vol. 201, No. 1-3, (1999), 102-104. https://doi.org/10.1016/S0304-8853(99)00065-7
57. Paul, P. S., "Design and Implementation of an Alternating Current Susceptometer for Measuring Brownian Relaxation Time of Magnetic Nanoparticles Suspended in a Liquid Medium", (2017). https://ir.library.oregonstate.edu/concern/graduate_projects/rr172296x